

# AN INVESTIGATION OF DAMPING MODIFICATION FACTORS CORRESPONDING TO DIFFERENT DAMPING RATIOS FOR SDOF SYSTEMS

*Emre Çağlar Çelik<sup>1</sup> and Onur Merter<sup>2</sup>*

1. *Politecnico di Milano, School of Civil, Environmental and Land Management Engineering, Milano, Italy; emrecaglar.celik@mail.polimi.it*

2. *İzmir University of Economics, Faculty of Engineering, Department of Civil Engineering, Balçova, İzmir, Turkey; \*onur.merter@ieu.edu.tr*

## ABSTRACT

The damping ratio is an important parameter in dynamic analyses and plays a key role in the design of building structures. Elastic response spectra are widely used in this design to describe the earthquake action in specific site classes. 5% damped response spectra are generally used for most of the conventional structures. However, other types of structures may not have a damping ratio of 5% and can have much lower or much larger damping ratios. The damping ratio is recommended at about 5% for concrete structures whereas it is estimated at 2% for steel structures. Tall slender buildings may have much lower damping ratios and low-rise buildings may be designed using much larger damping ratios than 5%. For these types of buildings, elastic response spectra are modified to account for different levels of damping ratios. This study proposes the damping modification factors (DMFs) which are computed using 5% damped response spectra as the benchmark. A strong ground motion set has been selected for the stiff site class and the displacement, pseudo-velocity, and pseudo-acceleration response spectra have been computed for single-degree-of-freedom (SDOF) systems. DMFs have been obtained in terms of these spectra and 3%, 10%, 20%, and 30% damping ratios have been considered. Variations of DMFs with different damping ratios have been obtained graphically. It can be seen from the results that DMFs are sensitive to the vibration period of the SDOF system.

## KEYWORDS

Damping modification factor, Damping ratio, Site class, Elastic response spectra, Strong ground motion, Single-degree-of-freedom system

## INTRODUCTION

Damping parameters play a significant role in dynamic analyses and the structural displacements decrease due to the increase in the damping. A 5% damping ratio is generally used for concrete structures and this ratio can vary depending upon many factors such as structure types, energy dissipation devices in buildings, changes in building heights and etc. [1-5]. High-rise buildings may have lower damping ratios whereas low-rise buildings have generally larger values. The damping ratio values decrease as the height of the building increases [4-6] and the estimation of the seismic response of tall buildings requires the damping ratio to be known [7]. In the seismic design of buildings in the United States, the damping ratio value is commonly recommended as lower than 2.5% for buildings higher than 150 m [7]. In addition to this, seismic energy dissipation devices may be installed in buildings to increase the damping ratio values and reduce structural damage [8].

Structures with these seismic energy devices generally have damping ratios above 10% for the first mode and much larger damping ratios for higher modes [4].

Response spectra are important tools in the seismic design of structures and engineers generally use 5%-damped pseudo-acceleration response spectra for typical structures. These spectra define the maximum responses of SDOF systems for specific ground motions. In widespread engineering applications, the most common method to define the seismic design loads that will affect an engineering structure is via the use of pseudo-acceleration spectral ordinates [5], and for this reason, the design acceleration spectra are described in many codes and regulations. In national and international seismic design codes, 5%-damped earthquake design spectra are usually generated for a specific territory using data on past earthquake ground motions.

For structural systems having damping ratios different than 5%, damping modification factors (DMFs) have been defined to estimate the seismic demands. These factors have been developed to make the conversion between a 5%-damped system and the other system having various damping ratios [5, 9]. The study to define DMF was first conducted by Newmark and Hall [10] and this pioneering study pointed out that these factors depend upon the natural vibration period of the system [5]. After Newmark and Hall's research, their relationship was adopted in ATC-40 [11] and FEMA 273 [12], [9]. Then, many seismic design codes such as UBC (1997) [13], Eurocode 8 (2004) [14], ASCE 7-05 (2006) [15], and NTCS-17 (2017) [16] proposed the DMF as a function of damping ratio. Priestley et al. [17] proposed a revision for the DMF relation in Eurocode 8 (2004) [14] for soil sites where forward directivity velocity pulse characteristics may be expected [9].

In this study, a total of 20 earthquake ground motion accelerograms are selected from the NGA-West2 strong ground motion database of the Pacific Earthquake Engineering Research Center (PEER) [18]. The site condition of the compiled accelerograms is defined in terms of the average shear wave velocity to the 30-meter depth of subsoil (in terms of  $V_{S30}$  Velocity). Site class ZD of the Turkish Building Earthquake Code (stiff soil with  $180 \text{ m/s} < V_{S30} \leq 360 \text{ m/s}$ ) is considered in the selection of accelerograms [19]. The fault rupture mechanism of the considered accelerograms is strike-slip and moment magnitudes ( $M_w$ ) are in the range of 6 to 7.9. Far-fault records are selected and the closest distances from the sites to the fault rupture planes (the rupture distances) are considered more than 15 km ( $R_{rup} > 15 \text{ km}$ ).

The displacement, pseudo-velocity, and pseudo-acceleration elastic response spectra of selected earthquakes are computed for 3%, 5%, 10%, 20%, and 30% damping ratios respectively. In the calculation process, SeismoSpect software is used [20]. DMFs are computed by considering 5%-damped response spectra as the benchmark and DMF relations are obtained depending upon the natural vibration period of the SDOF system. 3%, 10%, 20%, and 30%-damped DMF graphs are created by considering the displacement, pseudo-velocity, and pseudo-acceleration response spectra, and the mean DMFs are indicated in the same diagrams. Variations of DMFs with different damping ratios are also obtained graphically within the study. These diagrams are constituted for constant natural vibration periods of  $T_r = 0.5 \text{ s}$ ,  $1.0 \text{ s}$ ,  $1.5 \text{ s}$ ,  $2.0 \text{ s}$ ,  $2.5 \text{ s}$ ,  $3.0 \text{ s}$ ,  $3.5 \text{ s}$ , and  $4.0 \text{ s}$  respectively. It can be seen from the results that DMFs are sensitive to the natural vibration periods of SDOF systems. Additionally, for a specific natural vibration period value, it can also be seen from the graphs that the mean DMFs generally tend to decrease with the increase in the damping ratio. This result is consistent with the basic property of the response spectra and it could be defined as follows: "Response spectra ordinates decrease for the increasing values of damping ratio".

In this study, DMFs are computed by only using the selected earthquake ground motion accelerograms recorded at stiff soil sites. More specifically, using a larger number of earthquake record data one can conclude more exact results about the DMF variation with the natural vibration period of the constant-damped SDOF system. Nevertheless, within the study, the DMF variation is investigated on a small scale and one of the important results can be given as the sensitivity of DMFs to changes in the vibration periods. Various general conclusions can also be drawn from this small-scale study. For example; if requested, one can directly compute the displacement, pseudo-velocity, and pseudo-acceleration elastic response spectra of SDOF systems having different damping ratios, from the DMF relations.

## DAMPING MODIFICATION FACTOR

The damping modification factor in terms of spectral displacement ( $DMF_d$ ) can be generally defined as [4, 5]:

$$DMF_d = \frac{S_d(T, \xi)}{S_d(T, \xi:5\%)} \quad (1)$$

where  $S_d(T, \xi)$  is the spectral displacement of a linear elastic SDOF system having the damping ratio of  $\xi$  and  $S_d(T, \xi:5\%)$  is the spectral displacement of the 5%-damped linear elastic SDOF system.  $T$  represents the natural vibration period of the system. The damping modification factor can also be obtained by using the spectral velocity  $PS_V(T, \xi:5\%)$  and the spectral acceleration  $PS_a(T, \xi:5\%)$ . In this conversion, the natural frequency  $\omega_n$  can be used, and multiplying  $S_d(T, \xi)$  by  $\omega_n$  one can obtain  $PS_V(T, \xi)$  (Equ. (2)). In a similar way,  $PS_a(T, \xi)$  can be obtained by multiplying  $S_d(T, \xi)$  by  $\omega_n^2$  (Equ. (3)).

$$DMF_V = \frac{PS_V(T, \xi)}{PS_V(T, \xi:5\%)} \quad (2)$$

$$DMF_a = \frac{PS_a(T, \xi)}{PS_a(T, \xi:5\%)} \quad (3)$$

In these equations,  $PS_V(T, \xi:5\%)$  and  $PS_a(T, \xi:5\%)$  represent the spectral velocity and spectral acceleration of the 5%-damped linear elastic SDOF system (pseudo-velocity and pseudo-acceleration). Damping modification factors ( $DMF_d$ ,  $DMF_V$ , and  $DMF_a$ ) in Equations (1-3) are defined to estimate the seismic demands of structural systems having damping ratios different than 5%. DMFs are developed to make the conversion between a 5%-damped system and the other system having various damping ratios such as  $\xi$  [5, 9].

### Damping modification factors in different seismic design codes

The study to define DMF was first conducted by Newmark and Hall [10] and this pioneering study pointed out that these factors depend upon the natural vibration period [5]. This study inspired scientists in this field and afterward, the adoption of DMFs to many seismic design codes was made [9]. The DMF in Eurocode 8 can be stated in terms of the viscous damping ratio  $\xi$  as follows [9, 14]:

$$DMF = \sqrt{\frac{10}{5+\xi}} \geq 0.55 \quad (4)$$

Priestley et. al suggested a revision for the DMF in Eurocode 8, especially for sites where forward directivity velocity pulse characteristics might be expected [9, 17, 21-25].

$$DMF = \left(\frac{7}{2+\xi}\right)^{0.25} \quad (5)$$

In the Chinese Standard (The Standard Code for Seismic Design of Buildings: GB 50011-2010), the seismic design response spectra are adjusted for different damping ratios by using the DMF in equation (6) [26]:

$$DMF = 1 + \frac{0.05-\xi}{0.08+1.6\xi} \geq 0.55 \quad (6)$$

In the Japanese Seismic Design Code, the damping correction (modification) factor is defined in terms of the viscous damping ratio  $\xi$  as follows [27]:

$$DMF = \frac{1.5}{(1+10\xi)} \geq 0.4 \quad (7)$$

These examples can be increased for DMFs and one can obtain different DMF relations in terms of the viscous damping ratio  $\xi$  from many different seismic design codes [9]. In Figure1, these

code-based DMF relations (in Equations 4-7) are presented based on different viscous damping ratios.

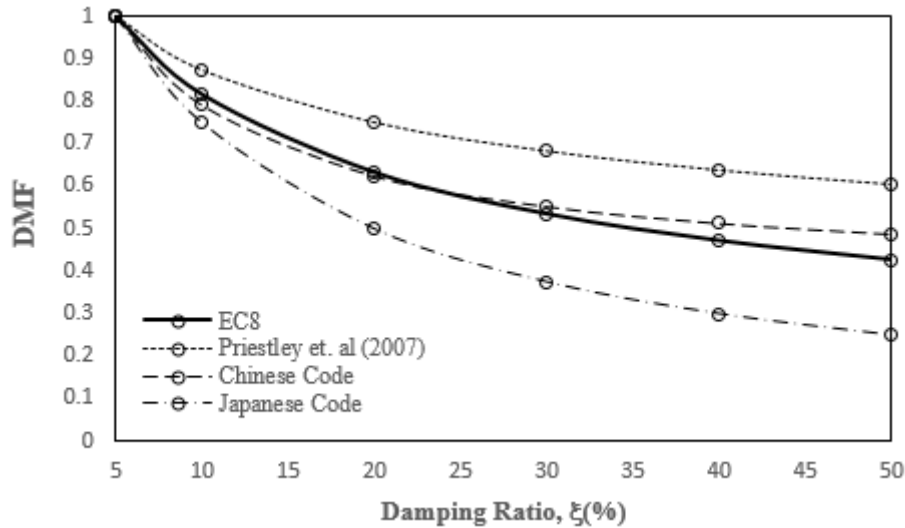


Fig. 1 – Damping modification factors (DMFs) according to Equations 4-7.

### SELECTED EARTHQUAKE GROUND MOTIONS

A total of 20 real earthquake records are selected from the NGA-West2 strong ground motion database of the Pacific Earthquake Engineering Research Center (PEER) [18]. Site class ZD (stiff soil with  $180 \text{ m/s} < V_{S30} \leq 360 \text{ m/s}$ ) is considered according to the Turkish Building Earthquake Code [19]. The fault rupture mechanism of the considered ground motion records is strike-slip. Moment magnitudes ( $M_w$ ) vary in the range of 6 to 7.9 and only far-fault records have been considered. Selected ground motion records are listed in Tables 1 and 2, respectively.  $R_{JB}$  is the Joyner-Boore distance,  $R_{rup}$  is the closest distance to the rupture plane, PGA is the peak ground acceleration, PGV is the peak ground velocity, PGD is the peak ground displacement,  $D_{a5-95}$  is the significant duration and  $I_a$  is the Arias intensity. The distribution of PGA of the selected records within the study is demonstrated in Figure 2 with respect to  $R_{rup}$ .

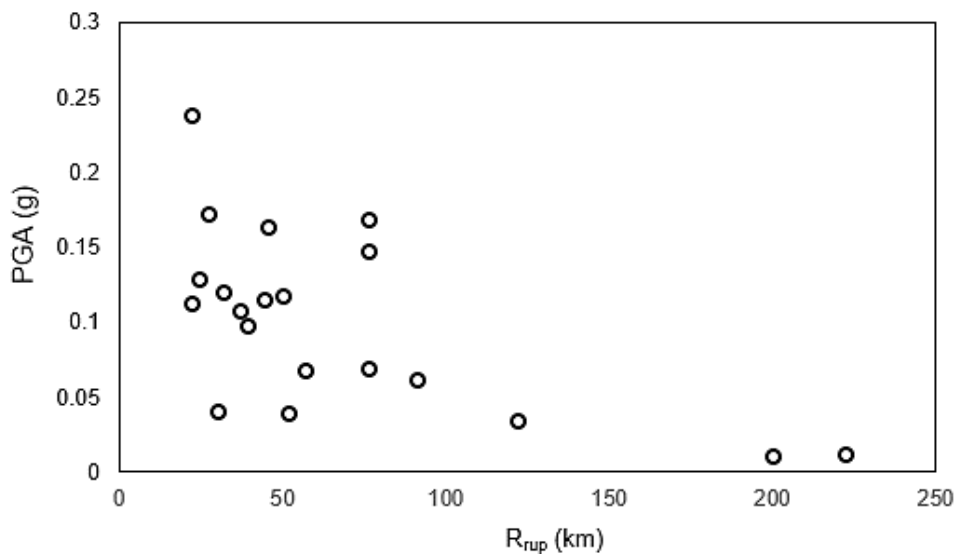


Fig. 2 – Distribution of PGA of the selected records with respect to  $R_{rup}$ .

Tab. 1 - Information on the selected ground motion records (Earthquakes 1-10) [18]

Record ID	Station Code	V <sub>s30</sub> (m/s)	Site Class	R <sub>JB</sub> (km)	R <sub>rup</sub> (km)	PGA (g)	PGV (cm/sec)	PGD (cm)	D <sub>a5-95</sub> (sec)	I <sub>a</sub> (m/s)
EQ 1	Ferndale City Hall	219.31	ZD	91.15	91.22	0.062	4.417	1.201	22.2	0
EQ 2	Ferndale City Hall	219.31	ZD	44.52	44.68	0.116	6.090	0.643	15.5	0.1
EQ 3	El Centro Array #9	213.44	ZD	56.88	56.88	0.068	6.438	4.213	37.2	0.1
EQ 4	Ferndale City Hall	219.31	ZD	26.72	27.02	0.172	38.242	14.593	19.4	0.5
EQ 5	El Centro Array #9	213.44	ZD	121.00	121.7	0.035	3.996	0.920	40.9	0.1
EQ 6	El Centro Array #9	213.44	ZD	45.12	45.66	0.163	24.928	10.180	49.3	0.2
EQ 7	LA - Hollywood Stor FF	316.46	ZD	222.42	222.42	0.012	3.188	1.313	26.3	0
EQ 8	LB - Terminal Island	217.92	ZD	199.84	199.84	0.011	2.710	1.770	37.9	0
EQ 9	Calipatria Fire Station	205.78	ZD	23.17	24.60	0.130	12.834	8.553	25.9	0.1
EQ 10	Coachella Canal #4	336.49	ZD	49.10	50.10	0.118	11.139	3.397	11.1	0.2

### Elastic response spectra of the selected earthquakes

Displacement, pseudo-velocity, and pseudo-acceleration response spectra of the selected earthquake ground motions are obtained within the study by using SeismoSpect software [20]. Viscous damping ratios are selected 3%, 5%, 10%, 20%, and 30%, respectively. As is seen from the mean spectra in Figure 3, spectral values generally decrease as the damping ratios increase. Using the natural frequency  $\omega_n$ , the pseudo-velocity  $PS_V$  can be obtained in terms of the spectral displacement  $S_d$  as [28]:

$$PS_V = S_d \omega_n \quad (8)$$

In the same way, the pseudo-acceleration  $PS_a$  can be determined by using the natural frequency  $\omega_n$  and the spectral displacement  $S_d$  as:

$$PS_a = S_d \omega_n^2 \quad (9)$$

As is known from structural dynamics, the dynamic equilibrium equation of a linear-elastic SDOF system can be written by [28]:

$$m\ddot{u} + c\dot{u} + ku = -m\ddot{u}_g \quad (10)$$

where  $m$  is the mass,  $u$  is the relative displacement,  $c$  is the damping coefficient,  $k$  is the stiffness and  $\ddot{u}_g$  is the acceleration of the ground motion. One can determine the peak displacement from this equation ( $u_{max}$ :  $S_d$ ) and the relation between the peak displacement and the natural vibration period  $T$  can be obtained (the displacement spectra). Using Equations (8) and (9), the pseudo-velocity  $PS_V$  and the pseudo-acceleration  $PS_a$  can be determined as in Figure 3.

Tab. 2 - Information on the selected ground motion records (Earthquakes 11-20) [18]

Record ID	Station Code	V <sub>s30</sub> (m/s)	Site Class	R <sub>JB</sub> (km)	R <sub>rup</sub> (km)	PGA (g)	PGV (cm/sec)	PGD (cm)	D <sub>a5-95</sub> (sec)	I <sub>a</sub> (m/s)
EQ 11	Delta	242.05	ZD	22.03	22.03	0.239	26.882	13.624	51.4	3.3
EQ 12	El Centro Array #13	249.92	ZD	21.98	21.98	0.113	15.370	8.246	21.6	0.3
EQ 13	Niland Fire Station	212.00	ZD	35.64	36.92	0.108	11.014	5.098	26.4	0.2
EQ 14	Plaster City	316.64	ZD	30.33	30.33	0.041	3.144	1.204	10.8	0.1
EQ 15	Victoria	242.05	ZD	31.92	31.92	0.121	7.435	2.166	34.3	0.3
EQ 16	SAHOP Casa Flores	259.59	ZD	39.10	39.30	0.098	7.353	1.542	11.0	0.1
EQ 17	Rio Dell Overpass - FF	311.75	ZD	76.06	76.26	0.069	8.037	3.603	12.4	0.2
EQ 18	Rio Dell Overpass. E Ground	311.75	ZD	76.06	76.26	0.169	11.005	3.250	12.3	0.4
EQ 19	Rio Dell Overpass. W Ground	311.75	ZD	76.06	76.26	0.147	10.965	3.114	10.8	0.4
EQ 20	APEEL 1E - Hayward	219.8	ZD	51.68	51.69	0.039	2.755	0.656	35.2	0

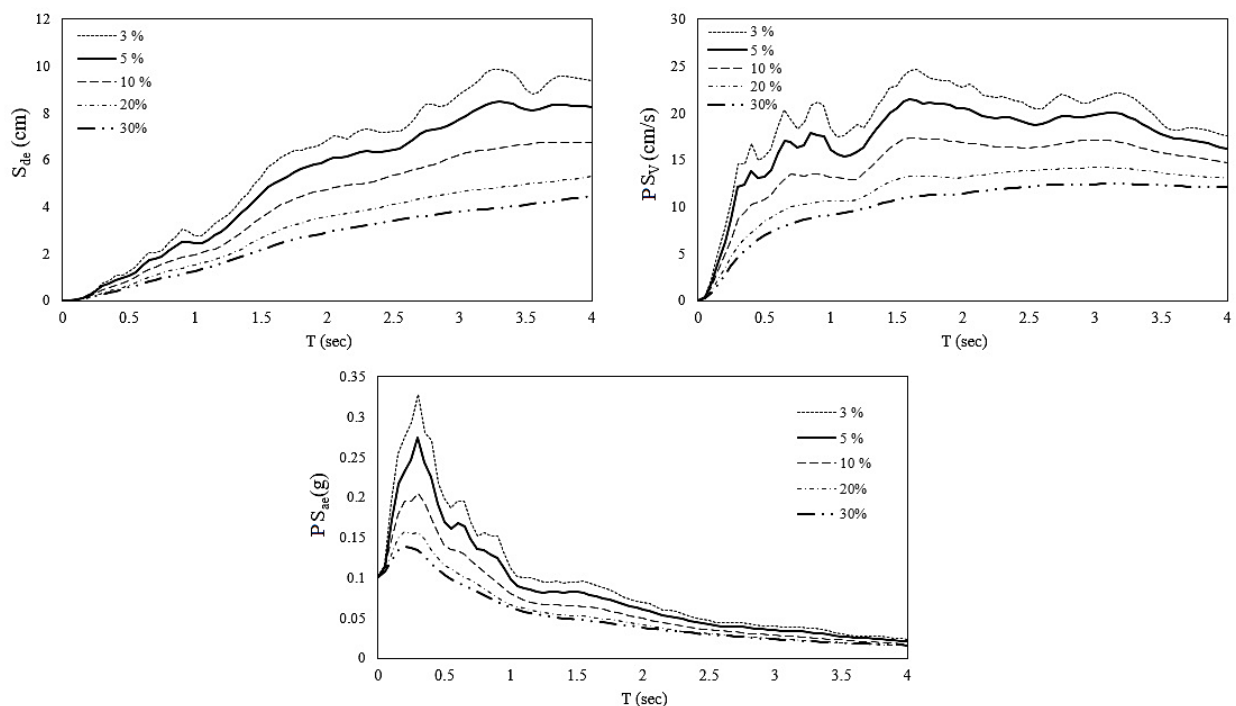


Fig. 3 – The mean elastic response spectra of the selected ground motions [in Tables 1 and 2] for 3%, 5%, 10%, 20%, and 30% viscous damping ratios.

**VARIATION OF DAMPING MODIFICATION FACTORS FOR SELECTED EARTHQUAKE GROUND MOTIONS**

In this study, DMFs have been computed for the selected earthquake ground motions. 5%-damped elastic response spectra have been selected as the benchmark and DMFs have been computed depending on the natural vibration period of the elastic SDOF system. 3%, 10%, 20%, and 30%-damped DMFs have been computed by considering the displacement ( $S_d$ ), pseudo-velocity ( $PS_v$ ), and pseudo-acceleration ( $PS_a$ ) response spectra, and the mean DMFs have been indicated in the same diagrams (Figures 4-6). The values of mean DMFs have been presented in Table 3.

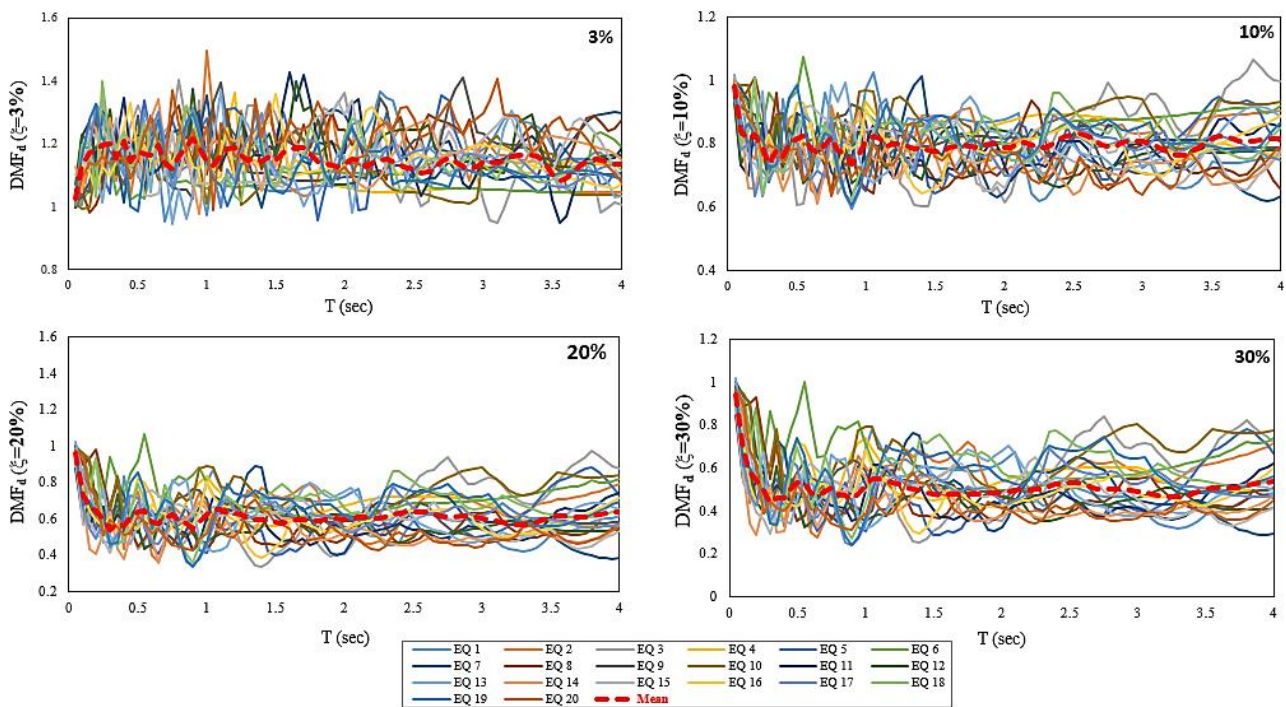


Fig. 4 – The variation of  $DMF_d$  (in terms of spectral displacement  $S_d$ ) for the selected earthquake ground motions [for  $\xi$ : 3%, 10%, 20%, and 30%].

Tab. 3 - Mean DMFs with respect to  $S_d$ ,  $PS_v$ , and  $PS_a$  (for different periods and  $\xi$ )

T	$\xi$ : 3%			$\xi$ : 10%			$\xi$ : 20%			$\xi$ : 30%		
	DMF $S_d$	DMF $PS_v$	DMF $PS_a$	DMF $S_d$	DMF $PS_v$	DMF $PS_a$	DMF $S_d$	DMF $PS_v$	DMF $PS_a$	DMF $S_d$	DMF $PS_v$	DMF $PS_a$
0.2 sec	1.215	1.179	1.177	0.829	0.775	0.838	0.643	0.556	0.671	0.546	0.444	0.595
0.5 sec	1.159	1.177	1.173	0.818	0.816	0.829	0.639	0.644	0.684	0.533	0.530	0.613
1.0 sec	1.146	1.143	1.138	0.807	0.820	0.822	0.625	0.658	0.682	0.521	0.567	0.635
1.5 sec	1.116	1.148	1.143	0.775	0.819	0.791	0.582	0.629	0.638	0.477	0.525	0.582
2.0 sec	1.108	1.137	1.132	0.789	0.822	0.808	0.595	0.641	0.675	0.483	0.555	0.625
3.0 sec	1.080	1.142	1.137	0.806	0.865	0.823	0.602	0.716	0.698	0.493	0.626	0.677
4.0 sec	1.084	1.136	1.130	0.817	0.906	0.844	0.639	0.806	0.749	0.540	0.746	0.776

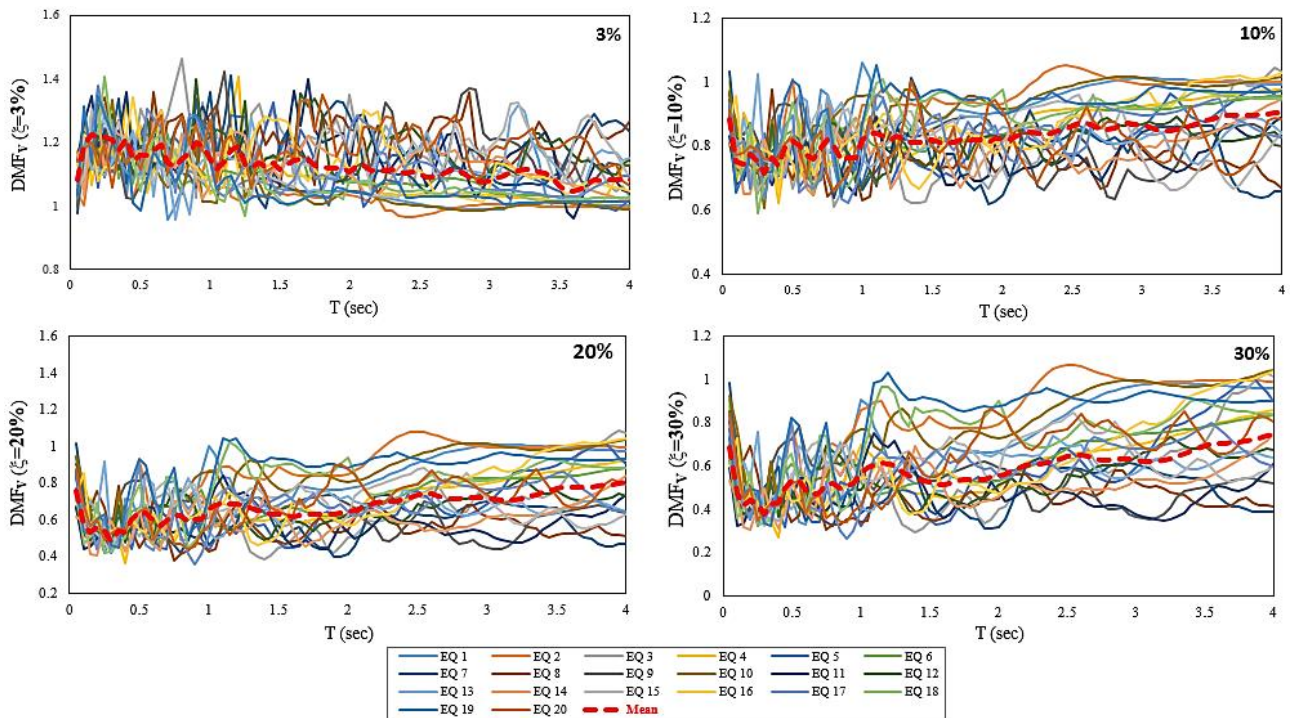


Fig. 5 – The variation of  $DMF_V$  (in terms of pseudo-velocity  $PS_V$ ) for the selected earthquake ground motions [for  $\xi$ : 3%, 10%, 20%, and 30%].

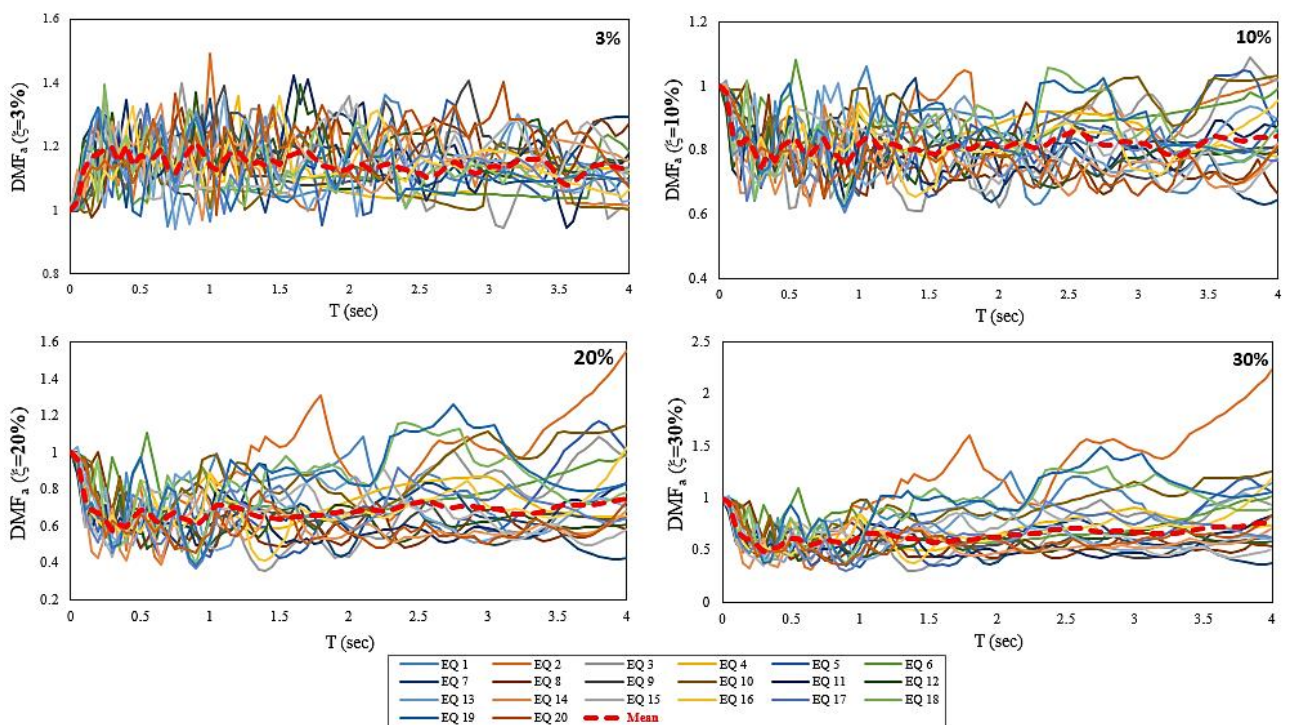


Fig. 6 – The variation of  $DMF_a$  (in terms of pseudo-acceleration  $PS_a$ ) for the selected earthquake ground motions [for  $\xi$ : 3%, 10%, 20%, and 30%].



### Mean DMF variations with respect to natural vibration periods

Mean DMF variations for the selected earthquake ground motions have been given in Figure 7. It can be clearly seen from the graphs that DMFs tend to decrease with the increase in viscous damping ratio. Mean DMF variations have been presented in terms of the ratios of displacement ( $S_d$ ), pseudo-velocity ( $PS_v$ ), and pseudo-acceleration ( $PS_a$ ) response spectra. The damping ratio effect on DMF values has been observed (Figure 7).

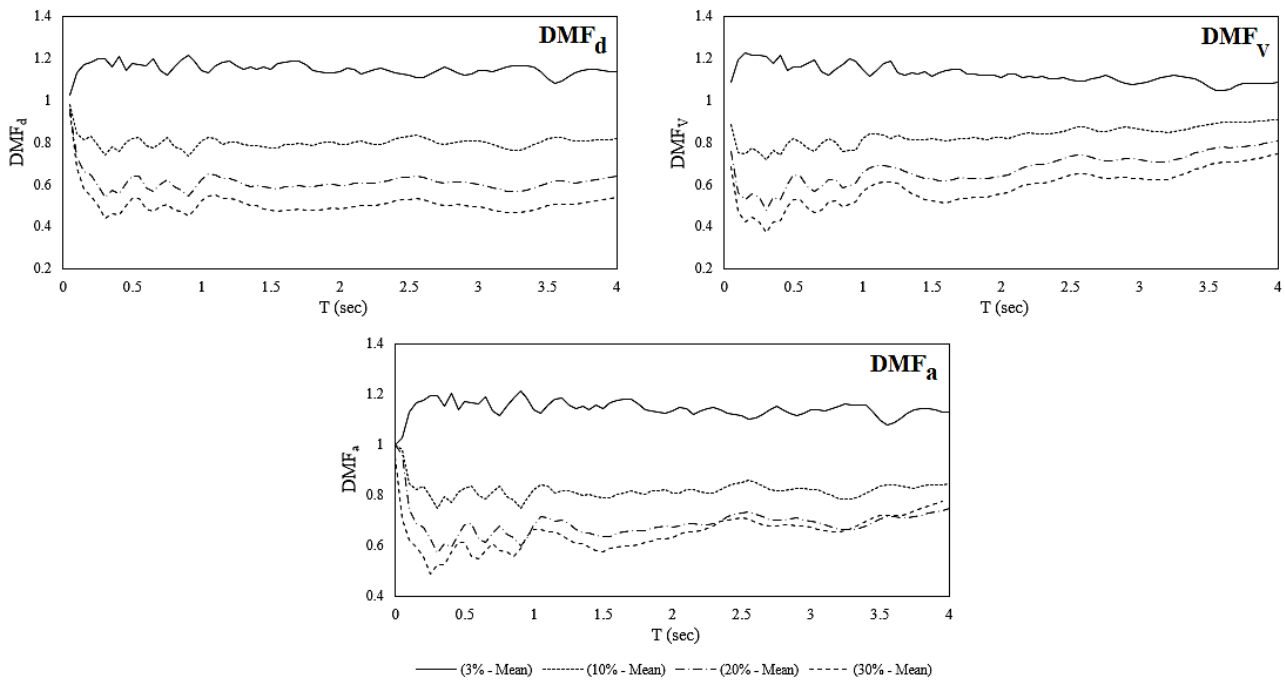


Fig. 7 – The variation of mean  $DMF_d$ ,  $DMF_v$ , and  $DMF_a$  with respect to the natural vibration periods and viscous damping ratios of 3%, 10%, 20%, and 30%.

### Mean DMF variations with respect to viscous damping ratios

In this study, Mean DMF variations for the selected earthquake ground motions have been presented in terms of viscous damping ratios, too. Once again, it is seen from the graphs that the mean DMFs tend to decrease with the increase in viscous damping ratios. In Figure 8, mean DMFs have been indicated for different viscous damping ratios of 3%, 10%, 20%, and 30%. In this figure, mean DMFs have been presented for all natural vibration periods of the elastic spectra. It can be seen from the figure that the mean DMF interval is scattered as the viscous damping ratio increases up to 30%. For the damping ratio of 3%, mean DMFs have been obtained very close to each other at different natural vibration periods.

$DMF_d$ ,  $DMF_v$ , and  $DMF_a$  variations with respect to the viscous damping ratios have been presented in Figure 9, for different natural vibration periods. In this figure mean DMFs have been considered for natural vibration periods of  $T_n=0.5$  s, 1.0 s, 1.5 s, 2.0 s, 2.5 s, 3.0 s, 3.5 s, and 4.0 s, respectively. Generally, for all periods, DMF values computed in terms of the ratios of spectral displacement, pseudo-velocity, and pseudo-acceleration response spectra ( $DMF_d$ ,  $DMF_v$ , and  $DMF_a$ ) tend to decrease for increasing values of viscous damping ratios (Figure 9). 5%-damped elastic response spectra have been selected as the benchmark within these computations (as given in Equations 1, 2, and 3).

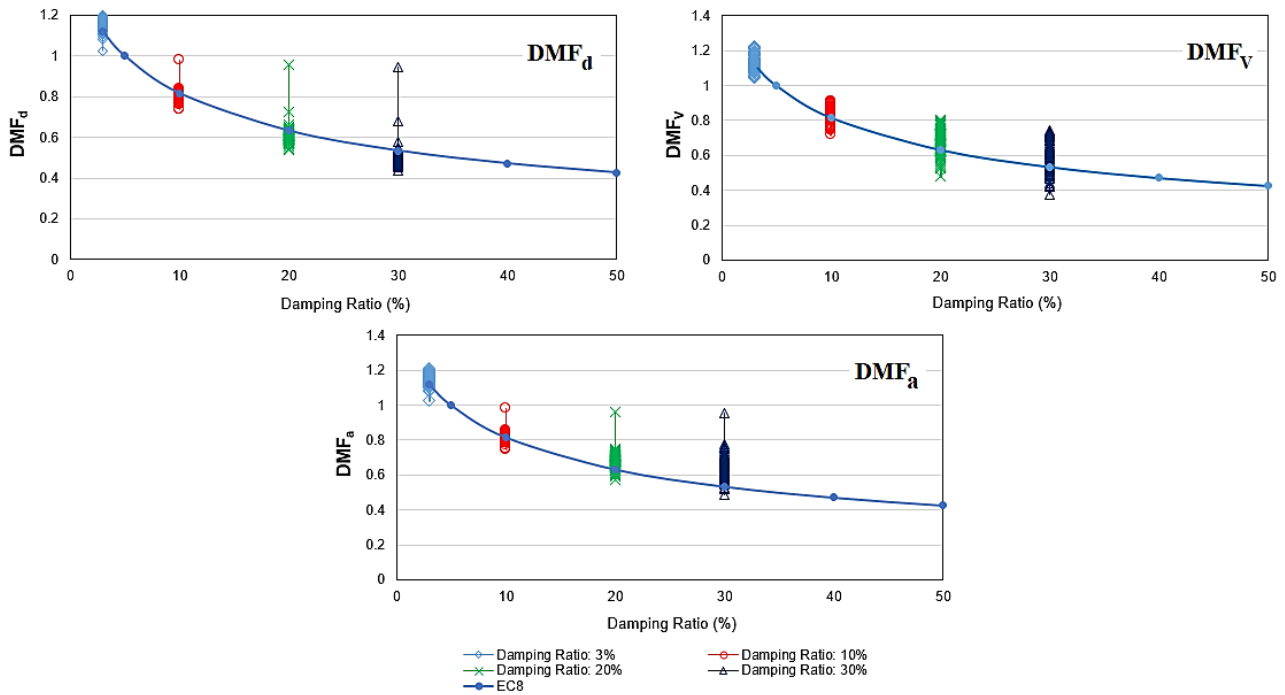


Fig. 8 – The variation of mean  $DMF_d$ ,  $DMF_V$ , and  $DMF_a$  with respect to the viscous damping ratios, and  $DMF$  variation according to Equation 4 (Equation in Eurocode 8).

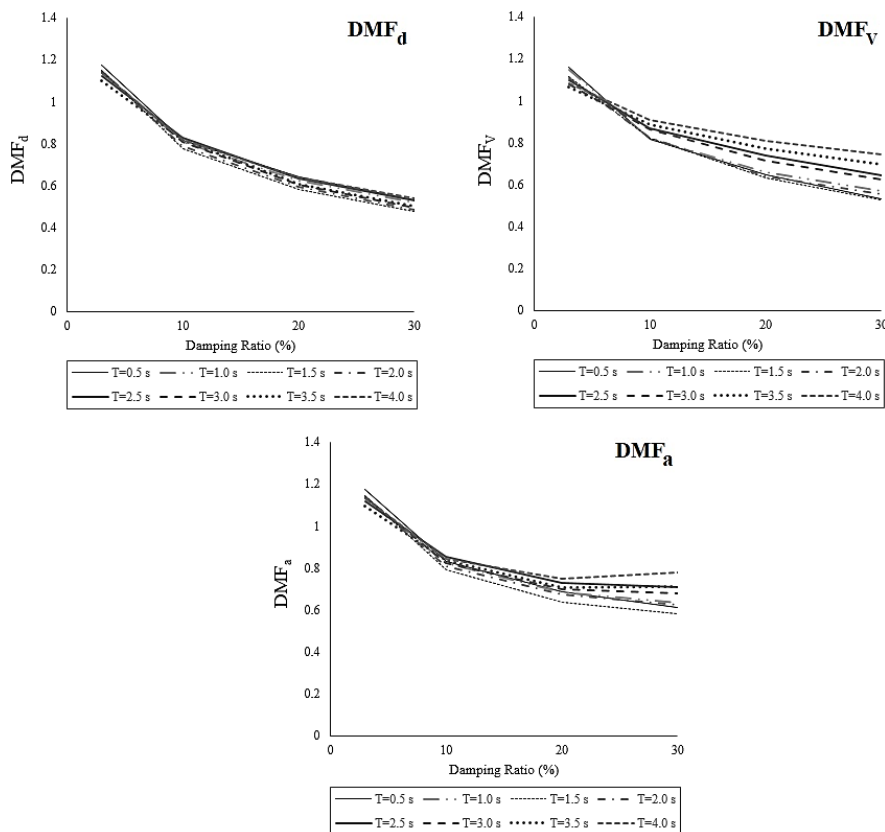


Fig. 9 –  $DMF_d$ ,  $DMF_V$ , and  $DMF_a$  variations with respect to the viscous damping ratios.

## CONCLUSION

The primary objective of this study is to investigate the damping modification factors, DMFs, for the selected earthquake ground motion accelerograms recorded at stiff soil sites with shear wave velocities less than 360 m/s. Computed DMFs modify 5%-damped spectral ordinates to estimate the seismic demands of structures whose damping ratio is different from 5%. DMFs have been obtained considering the displacement, pseudo-velocity, and pseudo-acceleration response spectra, and 3%, 10%, 20%, and 30% damping ratios have been considered. DMFs have been computed depending upon the natural vibration period of the elastic SDOF system, and variations of DMFs for different damping ratios have also been obtained graphically. It is seen from the graphs that DMFs are sensitive to the natural vibration periods of SDOF systems, and generally tend to decrease with the increase in the viscous damping ratio. The following conclusions can be drawn from the results of this study:

- DMFs have been obtained greater than 1.0 for 3% damping ratio whereas they have been obtained lower than 1.0 for all damping ratios greater than 5% (for damping ratios of 10%, 20%, and 30%). This is a natural result since DMFs are based on spectral values and since the displacement, pseudo-velocity, and pseudo-acceleration response spectra ordinates decrease with the increase in viscous damping ratios. As known, the DMF is the dimensionless ratio, and generally, 5%-damped spectral values are considered the benchmark. Therefore, when DMF is computed for structures like 3%-damped systems whose damping ratio is lower than 5% since the lower 5%-damped spectral value is in the denominator, the DMF is obtained greater than 1.0.
- For a constant natural vibration period of the SDOF system, it has been observed that the mean DMFs have decreased as the damping ratio has increased. Generally, between 3%- and 10%-damped systems, the difference in the mean DMFs has been obtained greater than that of the others.
- For longer natural vibration periods (especially for period values greater than 1.0 sec), the mean DMFs of the selected earthquake ground motions have been observed as tending to be nearly constant. For systems that have shorter natural vibration periods (especially for periods shorter than 0.3 sec), the mean DMFs have been observed as fluctuating.
- Mean DMF variations for the selected earthquake ground motions with respect to the viscous damping ratios have been obtained as compatible with the code-based DMF relations.

DMFs have been computed by only using the selected earthquake ground motion accelerograms recorded at stiff soil sites (on a small scale), within this study. More specifically, using a larger number of earthquake record data one can conclude more exact results about the DMF variation with the natural vibration period of the constant-damped SDOF systems.

## REFERENCES

- [1] Chowdhury I, Dasgupta, SP, 2003. Computation of Rayleigh Damping Co-efficient for Large Systems. *Electronic Journal of Geotechnical Engineering*, vol.43: 6855-6868.
- [2] Mario P, 2004. *Structural Dynamics: Theory and Computation*, 2nd Edn. CBS Publishers and Distributors, New Delhi.
- [3] Chopra AK, 2006. *Dynamics of Structures*, 3rd Edn. Wiley, London.
- [4] Conde-Conde J, Benavent-Climent A, 2019. Construction of Elastic Spectra for High Damping. *Engineering Structures*, vol.191: 343-357.
- [5] Davalos H, Miranda E, Bantis J, Cruz C, 2022. Response Spectral Damping Modification Factors for Structures Built on Soft Soils. *Soil Dynamics and Earthquake Engineering*, vol.154, <https://doi.org/10.1016/j.soildyn.2022.107153>.

- [6] Ha T, Shin S-H, Kim H, 2020. Damping and Natural Period Evaluation of Tall RC Buildings Using Full-Scale Data in Korea. *Applied Sciences*, vol.10(5): 1568, <https://doi.org/10.3390/app10051568>.
- [7] Cruz C, Miranda E, 2017. Evaluation of Damping Ratios for the Seismic Analysis of Tall Buildings. *Journal of Structural Engineering*, vol.143(1): 04016144, DOI:10.1061/(ASCE)ST.1943-541X.0001628.
- [8] Hernandez F, Astroza R, Beltran JF, Belmar L, 2020. A Damper-Spring Device for Seismic Energy Dissipation in Buildings. 17<sup>th</sup> World Conference on Earthquake Engineering, 17WCEE, Paper No: C001492, Sendai, Japan.
- [9] Sheikh MN, Tsang H-H, Yaghmaei-Sabegh S, Anbazhagan P, 2013. Evaluation of Damping Modification Factors for Seismic Response Spectra. Australian Earthquake Engineering Society 2013 Conference, November 15-17, Hobart, Tasmania.
- [10] Newmark NM, Hall WJ, 1973. Procedures and Criteria for Earthquake Resistant Design. Building Practices for Disaster Mitigation, Building Science Series, vol. 46, National Bureau of Standards: Washington, DC. P. 209-23.
- [11] ATC-40, 1996. Seismic Evaluation and Retrofit of Concrete Buildings. Applied Technology Council, Redwood City, CA.
- [12] FEMA-273, 1997. NEHRP Guidelines for the Seismic Rehabilitation of Buildings. Federal Emergency Management Agency, Washington, DC, USA.
- [13] UBC, 1997. Uniform Building Code. International Conference of Building Officials, Whittier, CA.
- [14] Eurocode 8 (EC8), 2004. Design of Structures for Earthquake Resistance, Part 1: General Rules, Seismic Actions and Rules for Buildings. EN 2004-1-1, CEN, Brussels.
- [15] ASCE 7-05, 2006. Minimum Design Loads for Buildings and Other Structures. American Society of Civil Engineers, 1801 Alexander Bell Drive, Reston, VA 20191, USA.
- [16] Mexico City Building Code, 2017. Complementary Technical Standards for Earthquake Design in Regulation of Constructions of the Federal District. NTCS-17, Official Gazette of the City of Mexico, Mexico.
- [17] Priestley MJN, Calvi GM, Kowalsky MJ, 2007. Displacement-Based Seismic Design of Structures. IUSS Press: Pavia, Italy.
- [18] PEER, 2022. Pacific Earthquake Engineering Research Center Strong Ground Motion Database. <http://ngawest2.berkeley.edu/>.
- [19] TBEC, 2018. Turkey Building Earthquake Code. Ministry of Public Works and Settlement, Ankara, Turkey.
- [20] SeismoSpect, 2022. Seismosoft, Earthquake Engineering Software Solutions, Pavia, Italy, <https://seismosoft.com/>.
- [21] Fernandez-Davila, VI, Mendo A., 2020. Damping Modification Factors for the Design of Seismic Isolation Systems in Peru, *Earthquake Spectra*, 1-28, DOI: 10.1177/8755293020926189.
- [22] Cicek K, Erkus B, 2019. Damping Reduction Factors for Maximum Rotated Spectra for Analysis of Base-Isolated Structures. 5<sup>th</sup> International Conference on Earthquake Engineering and Seismology (5ICEES), 8-11 October, Ankara, Turkey.
- [23] Cardone D, Dolce M, Rivelli M, 2009. Evaluation of Reduction Factors for High-Damping Design Response Spectra. *Bulletin of Earthquake Engineering*, vol.7, 273-291.
- [24] Daneshvar P, Bouaanani N, Goda K, Atkinson GM, 2017. Damping Modification Factors for Deep Inslab and Interface Subduction Earthquakes. 16<sup>th</sup> World Conference on Earthquake, Paper No. 2827, January 9-13, Santiago, Chile.
- [25] Daneshvar P, Bouaanani N, Goda K, Atkinson, GM, 2016. Damping Reduction Factors for Crustal, Inslab, and Interface Earthquakes Characterizing Seismic Hazard in Southwestern British Columbia, Canada. *Earthquake Spectra*, vol.32(1), 45-74, <https://doi.org/10.1193/061414EQS086M>.
- [26] GB 50011, 2010. Code for Seismic Design of Buildings. China Architecture & Building Press, Beijing, China.
- [27] BCJ, 1997. Structural Provisions for Building Structures. 1997 Edn-Tokyo: Building Center of Japan [in Japanese].
- [28] Chopra AK, 1995. Dynamics of Structures, Theory and Applications to Earthquake Engineering, Prentice Hall, Upper Saddle River, N.J.